MedChemComm

RESEARCH ARTICLE

View Article Online
View Journal

Cite this: DOI: 10.1039/c8md00313k

Search for a 5-CT alternative. *In vitro* and *in vivo* evaluation of novel pharmacological tools: 3-(1-alkyl-1*H*-imidazol-5-yl)-1*H*-indole-5-carboxamides, low-basicity 5-HT$_7$ receptor agonists†

Gniewomir Latacz, ‡*[a] Adam S. Hogendorf, ‡[b] Agata Hogendorf,[b] Annamaria Lubelska,[a] Joanna M. Wierońska,[b] Monika Woźniak,[bc] Paulina Cieślik,[b] Katarzyna Kieć-Kononowicz,[a] Jadwiga Handzlik[a] and Andrzej J. Bojarski[b]

Received 23rd June 2018,
Accepted 21st September 2018

DOI: 10.1039/c8md00313k

rsc.li/medchemcomm

Close structural analogues of 5-carboxamidotryptamine (5-CT) based on the newly discovered indole–imidazole scaffold were synthesized and evaluated to search for a 5-HT$_7$ receptor agonist of higher selectivity. *In vitro* drug-likeness studies and *in vivo* pharmacological evaluation of potent and selective low-basicity 5-HT$_7$ receptor agonists, previously published **7** (3-(1-ethyl-1*H*-imidazol-5-yl)-1*H*-indole-5-carboxamide, AH-494) and **13** (3-(1-methyl-1*H*-imidazol-5-yl)-1*H*-indole-5-carboxamide), have supported their usefulness as pharmacological tools. Comprehensive *in vitro* comparison studies between **7**, **13** and the commonly used 5-CT showed their very similar ADMET properties. Compound **7** at 1 mg kg^{-1} reversed MK-801-induced disruption in novel object recognition in mice and alleviated stress-induced hyperthermia (SIH) at high doses. Taking into account both *in vitro* and *in vivo* data, **7** and **13** may be considered as alternatives to 5-CT as pharmacological tools with important additional benefit associated with their low-basicity: high selectivity over 5-HT$_{1A}$R.

Introduction

The 5-HT$_7$ receptor (5-HT$_7$R), which was discovered independently by three teams in 1993, is the most recent one to be identified in the human serotonin system.[1–6] To date, extensive studies on 5-HT$_7$R have indicated its role in CNS development, circadian rhythm, memory and learning, thermoregulation, locomotion, hormonal regulation, hippocampus activity and mood control, as well as the pathophysiology of migraine, pain, depression and epilepsy.[1–6] Unfortunately, despite its possible therapeutic potential, no selective 5-HT$_7$R drug has yet been introduced to the market. Interestingly, the results obtained from animal models support the possible therapeutic applications of both 5-HT$_7$R agonists and antagonists.[1] For instance, the symptoms observed in an animal model caused by brain molecular alterations specific for Rett syndrome (RTT) were relieved after seven days of 5-HT$_7$R stimulation.[7,8] The selective activation of 5-HT$_7$R was also found to be beneficial in an animal model of fragile X syndrome (FXS), which is one of the genetic causes of intellectual disability and autism.[9] Investigations examining the long-term consequences of 5-HT$_7$R stimulation in adolescent rats have indicated plastic rearrangements within forebrain networks, accounting for long-lasting behavioral changes.[10] Pharmacological blockade of 5-HT$_7$R produced strong antidepressant-like response more rapidly than the classic antidepressant fluoxetine.[1–6]

Great efforts have been exerted by several research groups to develop new therapeutics and better molecular probes acting as selective 5-HT$_7$R ligands.[6] A few 5-HT$_7$R agonists have been used to date as tool compounds (Table 1), including the long-chain diphenylpiperazine, *e.g.*, LP-211 (**1**), and its low-weight metabolite RA-7 (**2**),[11] as well as several small molecules: pyrazoles AS-19 (**3**),[12] E-55888 (**4**)[13] and 5-carboxamidotryptamine (5-CT) (**5**)[14] (Fig. 1). However, due to their poor selectivity (RA-7, 5-CT),[15] low metabolic stability (LP-211),[16,17] failure to induce a full functional agonistic

[a] *Department of Technology and Biotechnology of Drugs, Jagiellonian University Medical College, Medyczna 9, 30-688 Kraków, Poland. E-mail: glatacz@cm-uj.krakow.pl; Tel: +48126205579*
[b] *Institute of Pharmacology, Polish Academy of Sciences, 12 Smętna Street, 31-343 Kraków, Poland*
[c] *Institute of Nuclear Physics, Polish Academy of Sciences Department of Experimental Physics of Complex Systems (NZ52), Radzikowskiego 152 Street, 31-342 Krakow, Poland*

† Electronic supplementary information (ESI) available. See DOI: 10.1039/c8md00313k

‡ Authors with equal contribution.

Table 1 Pharmacological *in vitro* profile of 5-HT_7R agonists

	Ligand/K_i [nM]									
Receptor	5-HT[14]	5-CT[14] (5)	AS-19 (ref. 15)	E-55888 (ref. 13)	LP-211 (ref. 11)	RA-7 (ref. 11)	AGH-107 (ref. 20) (6)	AH-494 (ref. 20) (7)	AGH-282 (13)	14	15
5-HT_{1A}	3.17	**0.3**	89.7	700	188	99	**1053**	**123**	**220**	**>10 000**	**>10 000**
5-HT_{2A}	11.55	**5012**	N.D.	>1000	626	1190	**>10 000**	**>10 000**	**>10 000**	**>10 000**	**>10 000**
5-HT_{5A}	251	**20**	98.5	N.D.	178	76	**>1000**[a]	**N.D.**	**N.D.**	**N.D.**	**N.D**
5-HT_6	98.41	**720**	N.D.	>1000	1571	596	**1673**	**>10 000**	**6910**	**7271**	**6062**
5-HT_7	8.11	**0.4**	0.6	2.5	0.6	1.4	**6**	**5**	**6**	**6417**	**161**
D_2	N.D.	**N.D.**	N.D.	N.D.	142	N.D.	**4847**	**>10 000**	**5561**	**>10 000**	**>10 000**

[a] Value estimated based on the results of a screening experiment.

response of intracellular signaling cascades (AS-19)[18] and low BBB permeability (5-CT and to some extent LP-211),[11] there is still a great demand for a "perfect" selective 5-HT_7 agonist, which could serve not only as a 5-HT_7R tool compound but also as a positron emission tomography (PET) radiotracer.[15–17,19] The ability to image serotonin 5-HT_7R in a living brain would allow direct assessments of the involvement of this receptor in neuropsychiatric diseases and possible therapies.[19]

The recently reported 5-(1*H*-indole-3-yl)-1-alkylimidazoles represent the first examples of low-basicity scaffolds exhibiting high affinity and selectivity for 5-HT_7R together with agonist function.[20] The hit compound AGH-107 (**6**) (Fig. 2) exhibited high affinity for and intrinsic activity at the receptor (K_i = 6 nM, EC_{50} = 19 nM, respectively). Compound **6** was also very selective over 5-HT_{5A}R, which is not a common feature of 5-HT_7R agonists (Table 1). Moreover, in drug-likeness studies *in vitro*, **6** was shown to be metabolically stable after incubation with human liver microsomes (Cl_{int} = 6.3 ml min^{-1} kg^{-1}) and exhibited very low toxicity in human embryonic kidney HEK-293 and *hepatoma* HepG2 cell lines and excellent water solubility. A PK experiment showed a high blood–brain barrier permeation, consistent with its high activity *in vivo*, where all three tested i.p. doses (0.5, 1 and 5 mg kg^{-1}) reversed MK-801-induced novel object recognition (NOR) impairment in mice.[20] The promising results highlighted the possible use of labeled **6** as a potential radioligand for both *in vitro* and *in vivo* studies.

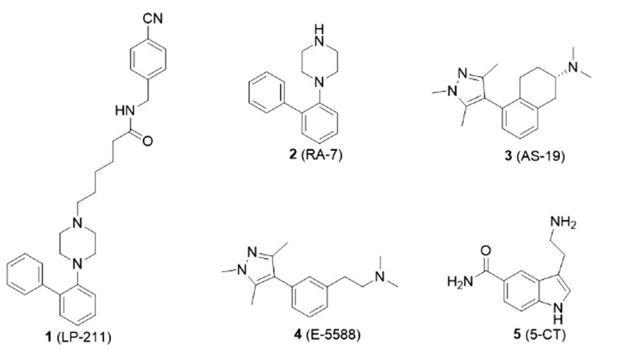

Fig. 1 The chemical structures of 5-HT_7R agonists used in neurobiological research.

During this study, our attention was focused on other potent compounds from that series: the 1*H*-indole-5-carboxamides AH-494 (**7**) (K_i = 5 nM, EC_{50} = 45 nM) and the newly obtained derivative AGH-282 (**13**) (K_i = 6 nM) (Fig. 2), which are close structural analogues of 5-carboxamidotryptamine (**5**) (Fig. 1), a molecular probe commonly used in serotonergic system-related research.[1,21]

Results and discussion

Chemistry

Aldehydes **8–10** were synthesized from the corresponding indoles *via* Vilsmeier–Haack formylation (Scheme 1). Compounds **11** and **12** which were the intermediates for the synthesis of **7** (AH-494) and **13**, respectively, as well as final compounds **14** and **15** were synthesized *via* van Leusen 3-component imidazole synthesis using the previously described protocol.[20] Compounds **7** and **13** were synthesized by a controlled hydrolysis of **11** and **12**, respectively.

In vitro

Radioligand displacement assays of compounds **7** and **13–15** showed, that only compounds with a carbonyl group (either ester or amide) at the 5th position of indole were found to possess significant affinity for the 5-HT_7R (Table 1). Compound **15** exhibited only medium binding to 5-HT_7R (K_i = 161 nM), while compound **13** was found only slightly less potent than **7** (K_i = 6 and 5 nM, respectively). Compounds **7** and **13** showed selectivity over 5-HT_{1A}R in opposition to 5-CT (25-fold and 37-fold *vs.* no selectivity at all).

The *in vitro* drug-likeness studies of **7**, **13** and the reference 5-HT_7R molecular probe **5** included the assessment of ADME-Tox parameters by using recombinant protein and enzymes (Pgp, CYP3A4, CYP2D6, CYP2C9), human (HLMs)

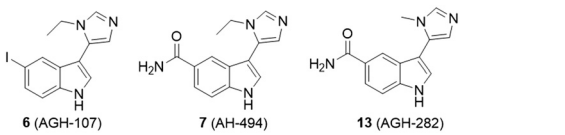

Fig. 2 The chemical structures of representative 5-(1*H*-indole-3-yl)-1-alkylimidazoles – the structurally novel molecular probes: AGH-107, AGH-282 and AH-494.

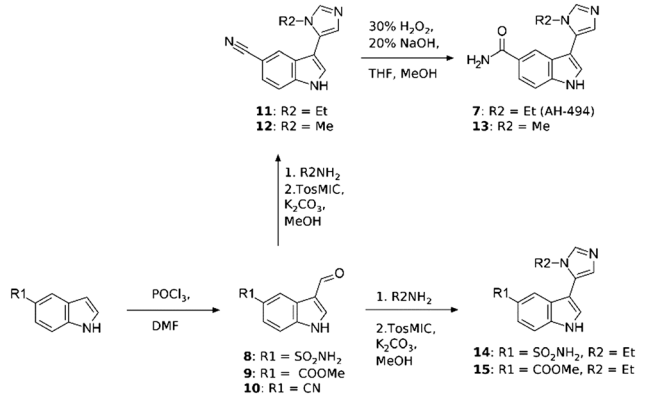

Scheme 1 Compounds **11**, **12**, **14** and **15** were synthesized *via* van Leusen multi-component reaction, while **7** and **13** were obtained by a controlled hydrolysis of **11** and **12**, respectively.

rat (RLMs) and mouse (MLMs) liver microsomes, human embryonic kidney (HEK-293), *neuroblastoma* (SH-SY5Y) and *hepatoma* (HepG2) eukaryotic cell cultures and the bacterial strain *Salmonella typhimurium*. The artificial membranes (PAMPA) were used for determination of passive membrane transport of **5** and **7**. The assay protocols and culture growth conditions were applied as described previously.[22,23]

The *in vivo* activity of CNS drugs depends on their penetration through biological membranes.[24] The parallel artificial membrane permeability assay (PAMPA) is commonly used in the early discovery and development process for the determination of compound passive transport. The Corning® PAMPA Plate System Gentest™ was used to determine the potential permeability of **5** and **7**. The method has been shown to provide good predictability of the membrane permeation and a high degree of correlation to the data obtained from absorption in the Caco-2 cell line.[25] The calculated permeability coefficient (Pe) for **5** (Pe = 3.54×10^{-6} cm s^{-1}) was slightly higher than for **7** (Pe = 2.78×10^{-6} cm s^{-1}) (Table 2). The results were compared to the references – highly permeable caffeine (Pe = 3.61×10^{-6} cm s^{-1}) and the low-permeable drug norfloxacin (Pe = 0.95×10^{-6} cm s^{-1}) and indicated very good passive transport of both **5** and **7** (Table 2).

The potential CNS bioavailability of **5**, **7** and **13** was also tested with respect to their influence on glycoprotein P (Pgp), the main efflux pump in both intestinal epithelium and the blood–brain barrier (BBB). The luminescence Pgp-Glo™ Assay System (Promega®) based on measurements of the changes in ATP consumed by Pgp[26] was used. The difference in the luminescent signal between samples treated with 100 μM of the selective Pgp inhibitor Na_3VO_4 (100% inhibition observed) and untreated samples represented the basal Pgp ATPase activity, which was considered herein as a negative control. The results were juxtaposed as the % of Pgp basal activity compared to the reference inhibitor (Na_3VO_4) and stimulator (verapamil, VL) (Fig. 3). Compounds **5** and **7** showed comparable, statistically significant inhibition effects on Pgp at 100 μM, with a decrease in ATP consumption to ~26 and ~19% of the basal activity, respectively (Fig. 3, Table 2). Despite the potentially enhanced risk of drug–drug interactions (DDIs), Pgp inhibition of CNS targeting compound **7** could exert a desirable effect by reducing its efflux from the BBB. No statistically significant influence of **13** on Pgp was also determined.

The metabolic stability of compounds **5**, **7** and **13** was evaluated *in silico* using MetaSite 5.1.1 (ref. 27) and *in vitro* using human, rat and mouse models with the respective liver microsomes, according to previously described methods and protocols.[22,23,28]

The *in silico* algorithm predicted, that the most likely metabolic site of **5** was the 2-aminoethyl chain, whereas the metabolic transformations for **7** and **13** were expected at the *N*-alkyl substituent at the imidazole ring (see Fig. S1 and S2 in ESI†).

The tested compounds were incubated with HLMs, RLMs and MLMs for 120 min at 37 °C in the presence of the NADPH regeneration system to determine their relative *in vitro* metabolic stability. UPLC analysis of the reaction mixtures collected after reaction with HLMs showed that approximately 20% of **5** was converted into two metabolites, M1 and M2 (see Fig. S3A in ESI†). However, due to the ambiguous MS spectrum of metabolite M1, only the M2 quasimolecular ion $[M + H]^+$ (m/z = 219.11) could be interpreted (see Fig. S4C and D in ESI†) (Table 2). The molecular mass of M2 (+14 units) suggests oxidation to the carbonyl group at the

Table 2 ADMET parameters of **5**, **7** and **13**

Parameter	Units	5	7	13
Permeability	(10^{-6} cm s^{-1} ± SD)	3.54 ± 8.2[a]	2.78 ± 9.2[a]	N.E.[d]
Pgp	(% of basal activity at 50 μM)	26.3 ± 12.0[a]	19.3 ± 12.3[a]	60.0 ± 16.0[a]
Metabolism with HLMs	(% of metabolized substrate)	26	N.A.[c]	N.A.[c]
Metabolism with RLMs	(% of metabolized substrate)	20	7	N.A.[c]
Metabolism with MLMs	(% of metabolized substrate)	2	14	9
CYP3A4 activity	(% of control ± SD at 10 μM)	95.7 ± 1.4[a]	2.9 ± 0.8[a]	29.37 ± 2.2[a]
CYP2D6 activity	(% of control ± SD at 10 μM)	108.3 ± 2.6[a]	43.4 ± 0.8[a]	55.0 ± 9.7[a]
CYP2C9 activity	(% of control ± SD at 25 μM)	78.7 ± 1.6[a]	104.2 ± 15.8[a]	37.20 ± 21.1[a]
HEK-293 viability	(% of control ± SD at 100 μM)	105.3 ± 7.0[b]	78.7 ± 16.8[b]	112.2 ± 5.2[b]
SH-SY5Y viability	(% of control ± SD at 100 μM)	91.0 ± 5.7[b]	106.7 ± 3.5[b]	88.4 ± 7.1[b]
HepG2 viability	(% of control ± SD at 100 μM)	101.3 ± 3.8[b]	78.7 ± 3.8[b]	82.2 ± 5.7[b]
ATP level in HepG2	(% of control ± SD at 100 μM)	N.E.[d]	101.6 ± 2.2[a]	N.E.[d]
Ames test	(No. of positive wells ± SD at 10 μM)	4.0 ± 2.9[a]	5.6 ± 1.2[a]	12.3 ± 1.5[a]

[a] Tested in triplicate. [b] Tested in quadruplicate. [c] Not applicable – no metabolism was observed. [d] N.E. – not examined.

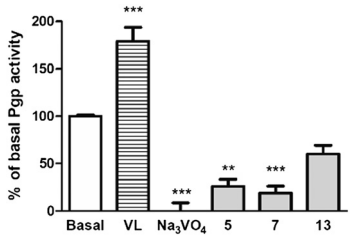

Fig. 3 The effect of the Pgp stimulator verapamil (VL) (200 μM), Pgp inhibitor Na_3VO_4 (100 μM) and compounds **5**, **7** and **13** on Pgp basal activity (basal). Data are presented as the mean ± SD. Statistical significance was evaluated by one-way ANOVA, followed by Bonferroni's comparison test (**$p < 0.01$, ***$p < 0.001$ compared with the negative control).

2-aminoethyl substituent as a metabolic pathway, which was also predicted *in silico* (see Fig. S2 in ESI†). UPLC analysis of the reaction mixtures of **7** and **13** after incubation with HLMs indicated their excellent metabolic stability, as no metabolites were present after incubation (see Fig. S3B and C in ESI†) (Table 2). Rodent models (mouse and rat) have shown similarities in the metabolism of **5** – only one metabolite with the same retention time (t_R = 1.62) was found after incubation with RLMs and MLMs (see Fig. S6A and S9A in ESI†). Comparison of the retention time of the metabolite obtained in rodent models with metabolite M1 (found after incubation with HLMs, t_R = 1.61) indicated that it could be the same molecule (see Fig. S4C, S7B and S10B in ESI†). However, as mentioned above, the molecular mass of this metabolite was not determined. The UPLC-MS spectra obtained from the reaction mixtures after incubation of **7** with RLMs and MLMs revealed the presence of the same metabolite with $t_R \sim 1.60$ min. and a molecular mass *m*/*z* of ~271 in both models (see Fig. S6B, S8C, S9B and S11C in ESI†). The molecular mass of the metabolite of compound **7** (+16 units) suggested that hydroxylation had occurred, presumably at the *N*-ethyl substituent, according to the fragmentation analysis and *in silico* data (see Fig. S1, S2 and S12 in ESI†). Moreover, **7** seemed to be slightly more stable in RLMs than in MLMs with 7% and 14% conversion, respectively (see Fig. S6B and S9B in ESI†) (Table 2). The results obtained for **13** after incubation with RLMs were similar to that for HMLs, as no metabolites were found (see Fig. S3C and S6C in ESI†) (Table 2). The UPLC-MS spectra obtained from the reaction mixture after incubation of **13** with MLMs revealed the presence of one metabolite with molecular mass *m*/*z* of ~274 and with 9% conversion of **13** (see Fig. S9C and S13 in ESI†). According to the fragmentation analysis and *in silico* data, the most probable metabolic pathway of **13** was a double hydroxylation (see Fig. S1, S2 and S14 in ESI†).

The cytochrome P450 isoforms 3A4 (CYP3A4), 2D6 (CYP2D6) and 2C9 (CYP2C9) are responsible for the metabolism of approximately 60–70% of all marketed drugs; the influence on CYP activity may be a source of potential dangerous DDI.[29] Luminescence-based CYP3A4, CYP2D6 and CYP2C9 P450-Glo™ assays (Promega®) were conducted to determine their activity at the presence of **5**, **7** and **13**. The assays were performed according to the manufacturer's protocols as described previously.[22,23] A strong cytochrome inhibition effect of **7** (IC_{50} = 0.31 μM), which is similar to the reference inhibitor ketoconazole (IC_{50} = 0.14 μM), was revealed (Fig. 4A) (Table 2). The CYP3A4 inhibition was also observed for **13** (IC_{50} = 3.53 μM) (Fig. 4A) (Table 2). Surprisingly, no effect on CYP3A4 activity was observed in the presence of **5** (Fig. 4A) (Table 2). An inhibition effects of **7** and **13** on CYP2D6 were also observed (IC_{50} = 7.47 and 27.60 μM, respectively), whereas slight CYP2D6 induction by **5** was observed at the highest doses (Fig. 4B) (Table 2). The highest inhibition effect on CYP2C9 was observed for **13** (~40% of the enzyme activity) only at the dose 25 μM (Fig. 4C) (Table 2). Thus, the *N*-substituted imidazole moiety of **7** and **13** is responsible for the interaction with cytochromes, as imidazole is the common molecular feature of many CYP inhibitors.[30]

In vitro safety profiling is an essential component of the drug discovery process, providing a reliable alternative to animal testing. The cytotoxicity, neurotoxicity, hepatotoxicity and mutagenicity of **5**, **7** and **13** were tested using HEK-293, SH-SY5Y, and HepG2 eukaryotic cell lines and the bacterial strain *Salmonella typhimurium*. The growth conditions and assay protocols have been described previously.[22,23] The colorimetric standard MTS assay allowed for the determination of eukaryotic cell viability after 72 h of incubation with **5**, **7** or **13**. A statistically significant influence on viability was

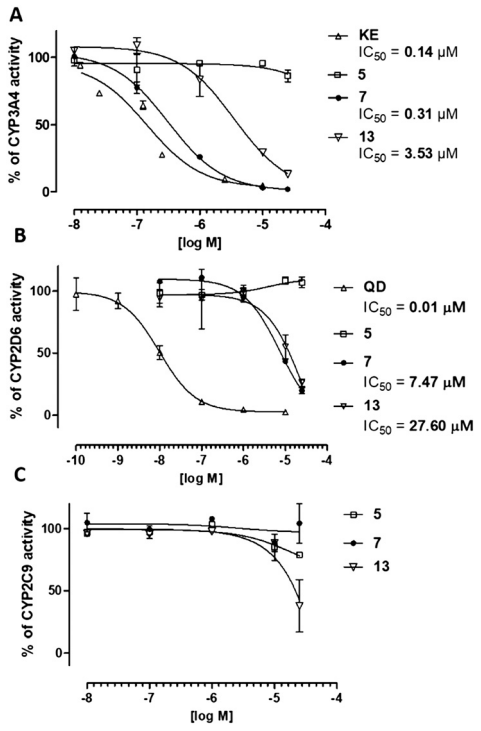

Fig. 4 The effect of ketoconazole (KE), **5**, **7** and **13** on CYP3A4 activity (A). The effect of quinidine (QD), **5**, **7** and **13** on CYP2D6 activity (B). The effect of **5**, **7** and **13** on CYP2C9 activity (C).

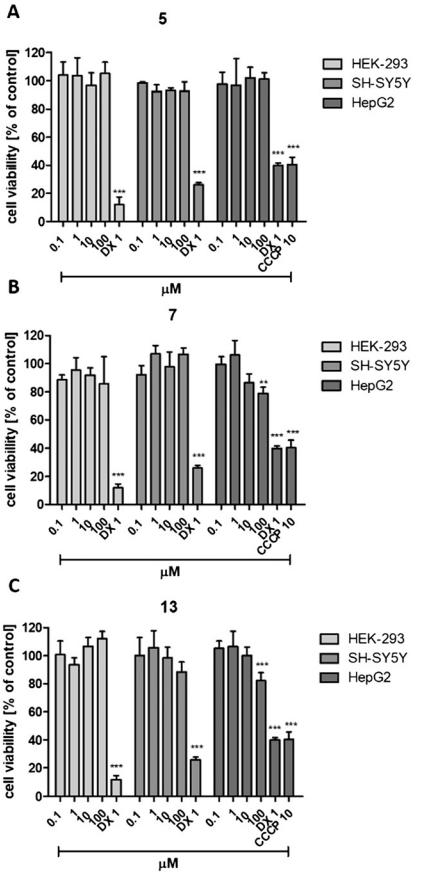

Fig. 5 The effects of doxorubicin (DX) and **5** (A), **7** (B) and **13** (C) on HEK-293, *neuroblastoma* SH-SY5Y and *hepatoma* HepG2 cell line viability after 72 h of incubation. The mitochondrial toxin carbonyl cyanide 3-chlorophenyl-hydrazone (CCCP) was used at 10 μM as an additional positive control for the *hepatoma* HepG2 cell line. Statistical significance was evaluated by one-way ANOVA, followed by Bonferroni's comparison test (**$p < 0.01$, ***$p < 0.001$ compared with the negative control).

shown for **7** and **13** in one (HepG2) among the three examined cell lines (Fig. 5). However, the decrease in HepG2 viability to ~80% was observed only for the highest dose of 100 μM (Fig. 5) (Table 2), suggesting a very weak toxicity of **7** and **13** in comparison to the effect of the references DX and CCCP, which decreased the cell viability to ~40% at 1 and 10 μM, respectively (Fig. 5). Potential hepatotoxic effects of **7** were ruled out in additional tests in which the ATP level was measured *via* luminescence after a short 3 h exposure of the cells to **7**. No influence of **7** on cell metabolism and mitochondrial respiration was observed, even at the highest dose (100 μM, Fig. 6).

The mutagenicity potential of **5**, **7** and **13** was evaluated using the Ames microplate fluctuation protocol (MPF),[31] as described previously.[22,23] The *Salmonella typhimurium* strain TA100 was used, which enables the detection of frame shift mutations. The number of revertants observed in the control (growth medium + 1% DMSO) allowed for determination of the medium control baseline (MCB). According to the assay kit manufacturer, a 2-fold increase over the MCB is considered a mutagen alert. The results were compared to the reference mutagen nonyl-4-hydroxyquinoline-*N*-oxide (NQNO) at 0.5 μM. Mutagenic potential of all compounds was not observed (Fig. 7).

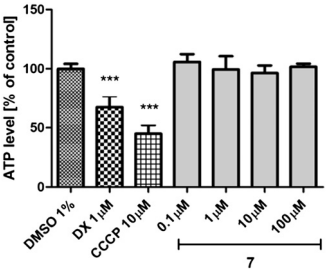

Fig. 6 The effects of doxorubicin (DX), mitochondrial toxin carbonyl cyanide 3-chlorophenylhydrazone (CCCP) and **7** on ATP levels in *hepatoma* HepG2 cells after 3 h of incubation.

In vivo

The *in vivo* evaluation of the biological activity of **7** included a novel object recognition (NOR) and stress-induced hyperthermia (SIH) assays. Compound **7** reversed MK-801-induced

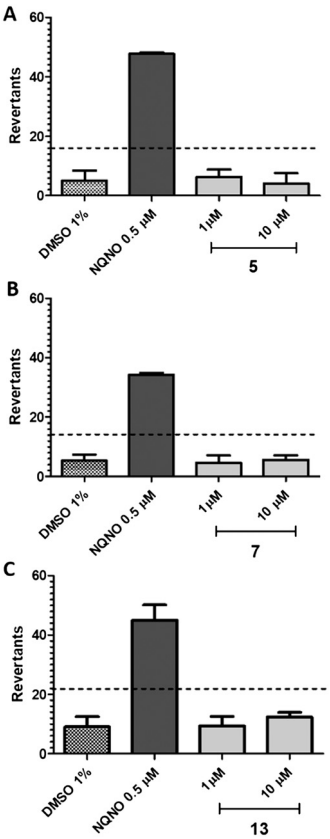

Fig. 7 Number of histidine prototrophy revertants of *Salmonella typhimurium* strain TA100 exposed to **5** (A), **7** (B) and **13** (C) or the reference mutagen nonyl-4-hydroxyquinoline-*N*-oxide (NQNO). The dashed line marks the 2-fold increase over MCB – considered a mutagen alert. The MCB corresponds to the mean number of revertants in the control plus one standard deviation.

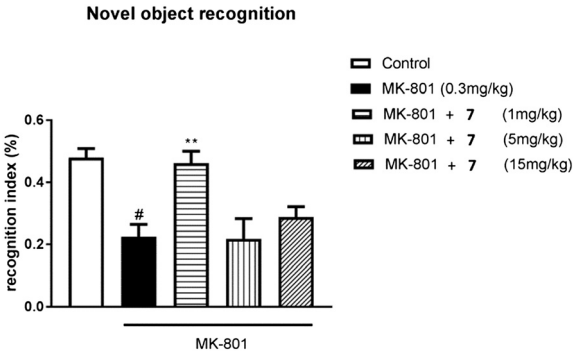

Fig. 8 Reversal of MK-801 induced disruption of novel object recognition. The results are presented as the means ± SEM. $N = 10$. $^{**}p < 0.01$. $N = 10$. $\#p < 0.001$ and $^{*}p < 0.01$.

disruption in the NOR test at relatively low doses (Fig. 8), supporting its potential to improve short-term working memory – however, this effect has also been observed for 5-HT_7R antagonists.[32] It is likely that the 5-HT_7R may play a different role in the acquisition and consolidation of recognition memory,[1,33] which could explain why the administration of both agonists and antagonists can lead to procognitive effects. The reverse dose-dependence can potentially be attributed to the activity of the compound at the 5-HT_{1A} receptor (or other targets), which may influence the effect of 5-HT_7R activation at the highest doses. Moreover, the activity of the compound was also evident in the SIH test, which reflects the autonomic response to stress in animals and is one of the most recognized tests for anxiety. However, the activity was observed only at the highest dose (Fig. 9).

Experimental

Chemicals

The reference compounds used during *in vitro* study, as follows: caffeine, norfloxacin, doxorubicin, carbonyl cyanide 3-chlorophenylhydrazone, ketoconazole, quinidine, nonyl-4-hydroxyquinoline-*N*-oxide were provided by Sigma-Aldrich (St. Louis, MO, USA). The references in Pgp assay: Na_3VO_4 and verapamil were provided by Promega (Madison, WI, USA).

All the chemicals for syntheses were supplied by the companies: Combi-Blocks, Inc. 7949 Silverton Avenue, Suite 915 San Diego, CA 92126 USA, Sigma-Aldrich Sp. z o.o. Poznan, Poland and Chempur, Jana Lortza 70A, 31-940 Piekary Śląskie.

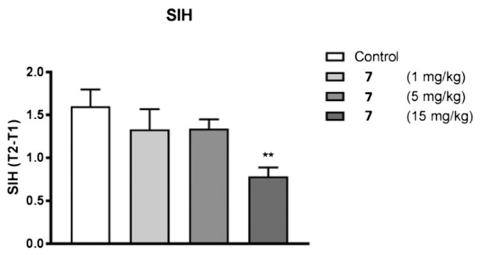

Fig. 9 The effect of **7** on stress-induced hyperthermia (SIH). The results are presented as the means ± SEM. $N = 10$. $^{**}p < 0.01$.

General procedures for the preparation of compounds 7–15

General procedure 1 for the synthesis of Indole-3-carboxaldehydes 8–10. Aldehydes were prepared as described previously.[20] The Vilsmeier–Haack reagent was generated by the addition of 2 ml of $POCl_3$ over the course of 15 minutes to 8 ml of dry DMF cooled in an ice-salt bath. After the addition was complete, the ice bath was removed and the contents of the flask were left to warm to room temperature over approx. 30 minutes. The substituted indole (21.9 mmol) was dissolved in 10 ml of DMF and added over a period of 15 minutes to the formylating mixture. The stirring was continued for an hour during which the flask contents were heated to 40 °C in a hot water bath. A total of 20 ml of 5 M NaOH was added, and the mixture was diluted with H_2O, quickly brought to a boil and left to cool slowly. The crystals were removed by filtration, washed with cold water and vacuum dried. The products thus obtained were in most cases sufficiently pure for the subsequent reactions. The impure aldehydes were recrystallized from ethanol–water mixtures.

General procedure 2 for the synthesis of 1-alkylimidazoles 11, 12, 14, 15. Van Leusen reaction was conducted as described previously.[20] Aromatic aldehyde (3 mmol) was mixed with amine (15 mmol) in 20 ml dry methanol. Reaction mixture was left overnight to complete the imine formation although it can be TLC monitored (SiO_2/$CHCl_3$). Anhydrous K_2CO_3 (3 mmol) and TosMIC (tosylmethylisocyanide, 3 mmol) were subsequently added. The mixture was stirred for an additional 8 hours, diluted with 50 ml H_2O, and extracted three times with 20 ml ethyl acetate. The combined extracts were washed twice with 20 ml H_2O, and once with 20 ml brine, treated with anhydrous magnesium sulfate and evaporated. The final products were purified by trituration under a 2 : 1 hexane : isopropanol mixture.

General procedure 3 for the synthesis of 3-(1-alkyl-1*H*-imidazol-5-yl)-1*H*-indole-5-carboxamides (7 and 13). Compounds were synthesized from appropriate nitriles (**11** and **12**, respectively), the cyanide group hydrolysis was accomplished according to a modified procedure outlined by Agarwal *et al.*[34] A suspension of the nitrile (3.4 mmol) in 1 ml MeOH and 5 ml THF was stirred in an ice-salt bath for 15 minutes until 0 °C was reached. Hydrogen peroxide (30% solution, 5.4 ml) was added dropwise keeping the temperature below 10 °C. Stirring was continued for 15 minutes and sodium hydroxide (20% solution, 5.4 ml) was added dropwise keeping temperature below 10 °C. The mixture was allowed to warm to room temperature and stirred for 24 hours. The product was extracted from the reaction mixture with chloroform–methanol mixture (9 : 1 v/v) and purified by trituration with acetone.

Analytical methods

UPLC/MS analysis was performed on Waters TQD spectrometer combined with UPLC Acquity H-Class with PDA eLambda

detector. Waters Acquity UPLC BEH C18 1.7 μm 2.1 × 50 mm chromatographic column was used, at 40 °C, 0.300 ml min^{-1} flow rate and 1.0 μL injection volume (the samples were dissolved in LC-MS grade acetonitrile, typically at a concentration of 0.1–1 mg ml^{-1} prior to injection). All mass spectra were recorded under electrospray ionization in positive mode (ESI^+) and chromatograms were recorded with UV detection in the range of 190–300 nm. The gradient conditions used were: 80% phase A (water + 0.1% formic acid) and 20% phase B (acetonitrile + 0.1% formic acid) to 100% phase B (acetonitrile + 0.1% formic acid) at 3.0 minutes, kept till 3.5 minutes, then to initial conditions until 4.0 minutes and kept for additional 2.0 minutes. Total time of analysis – 6.0 minutes. ^1H, ^{13}C NMR and 2D NMR spectra were recorded on Bruker Avance III HD 400 NMR and Bruker AVANCE 500 MHz spectrometers. All samples were dissolved in DMSO-d_6 with TMS as the internal standard.

Pharmacology

Compounds **13–15** were tested in a radioligand binding assays to determine their affinity for five receptors: 5-HT_{1A}, 5-HT_{2A}, 5-HT_6, 5-HT_7 and D_2. The assays were performed *via* the displacement of the respective radioligands from cloned human receptors, all stably expressed in HEK-293 cells (except for 5-HT_{2A} which was expressed in CHO cells): [^{3}H]-8-OH-DPAT for 5-HT_{1A}R, [^{3}H]-ketanserin for 5-HT_{2A}R, [^{3}H]-LSD for 5-HT_6R, [^{3}H]-5-CT for 5-HT_7R and [^{3}H]-raclopride for D_2R. The detailed procedure can be found in ESI.†

PAMPA

Pre-coated PAMPA Plate System Gentest™ (Corning, Tewksbury, MA, USA) was used for permeability evaluation. All experiments were performed as described before.[22,23] The calibration curves of 5-HT_7R agonists **5** and **7** and reference substances were prepared using capillary electrophoresis (CE) system P/ACE MDQ (Beckman Coulter, Fullerton, CA, USA), controlled by 32 Karat Software version 8.0, and equipped with diode-array detector (DAD).

Influence on Pgp activity

The influence of **5**, **7** and **13** on glycoprotein P (Pgp) activity was estimated using the luminescent Pgp-Glo™ Assay System (Promega, Madison, WI, USA) as described previously.[23] The reference inhibitor Na_3VO_4 was used in 100 μM concentration and reference stimulator verapamil in 200 μM, according to the manufacturer's recommendations. Compounds were examined at 100 μM. All compounds were incubated with Pgp membranes for 40 minutes at 37 °C in triplicate. GraphPad Prism™ software (version 5.01, San Diego, CA, USA) was used to calculate statistical significance.

Metabolic stability

Human (HLMs), rat (RLMs) and mouse liver microsomes (MLMs) were purchased form Sigma-Aldrich (St. Louis, MO, USA). The NADPH regeneration system was purchased from Promega® (Madison, WI, USA). All experiments were performed as described before.[20,22,23]

Influence on CYP3A4 and CYP2D6 activity

The luminescent CYP3A4 P450-Glo™, CYP2D6 P450-Glo™ and CYP2C9 P450-Glo™ assays and protocols were provided by Promega® (Madison, WI, USA). All experiments were performed as described before.[20,22,23] Each compound was tested in triplicate at the final concentrations similar for all CYP3A4, CYP2D6 and CYP2C9 assays in range from 0.01 to 25 μM. The luminescent signal was measured by using a microplate reader EnSpire PerkinElmer (Waltham, MA, USA).

Safety

Human embryonic kidney HEK-293 cell line (ATCC® CRL-1573™) was kindly donated by Prof. Dr. Christa Müller (Pharmaceutical Institute, Pharmaceutical Chemistry I, University of Bonn). *Hepatoma* HepG2 (ATCC® HB-8065™) cell line was kindly donated by the Department of Pharmacological Screening, Jagiellonian University Medical College. SH-SY5Y (ATCC® CRL-2266™) cell line was purchased from ATCC. The cell cultures' growth conditions were applied as described before.[20,22,23] The CellTiter 96® AQueous Non-Radioactive Cell Proliferation Assay (MTS) was purchased from Promega (Madison, WI, USA). The absorbance of the samples was measured using a microplate reader EnSpire (PerkinElmer, Waltham, MA USA) at 490 nm. The reference compounds CCCP (10 μM) and DX (1 μM) as well as compounds **5**, **7** and **13** (0.1–100 μM) were tested in four repetitions.

The CellTiter-Glo Luminescent Cell Viability Assay for ATP-level assessment was purchased from Promega® (Madison, WI, USA). The ATP level was measured as described previously after 3 h of HepG2 cells' exposure on compound **7** tested at three concentrations (1, 10 and 100 μM), and on the reference compounds CCCP (10 μM) and DX (1 μM).[22,23] The luminescence signal was measured with a microplate reader EnSpire (PerkinElmer, Waltham, MA USA) in luminescence mode. The assay was performed in quadruplicate.

The *Salmonella typhimurium* TA100 strain with base pair substitution (*hisG46* mutation, which target is GGG) was purchased from Xenometrix, Allschwil, Switzerland, and has been used in mutagenicity Ames 384 – well microtiter assay. All experiments were performed as described before.[22,23]

GraphPad Prism™ software (version 5.01, San Diego, CA, USA) was used to calculate statistical significance in all safety experiments.

Novel object recognition experiment

The method was performed according to Nilsson *et al.*[35] The animals were trained and tested in a black, plastic, open field (50 × 30 cm, 35 cm high). The open field was in a dark room illuminated only by a 25 W bulb. On the first day (adaptation) the animals were allowed to explore the open field for 10 min. On the next day (training, T1) the

animals were administered the tested drugs, placed in the apparatus and allowed to explore two identical objects (a red, glass cylinder, 6.5 cm in diameter, 4.5 cm high). For the retention trial (T2) conducted one hour later, one of the objects presented in T1 was replaced with a novel object (a transparent glass elongated sphere-like object with an orange cap). The duration of exploration of each object (*i.e.*, sitting in close proximity to the objects or sniffing or touching them) during 5 min time was video recorded and measured separately by a trained observer. All drugs were administered before the training (T1) session. MK-801 (0.3 mg kg^{-1}, i.p.) was given 30 min before the session. Investigated compounds were administered 60 min before MK-801.

The modified stress-induced hyperthermia in singly-housed mice

Each experimental group consisted of eight to ten animals in a modified stress-induced hyperthermia (SIH) test. The animals were housed individually in a 26 × 21 × 14 cm Macolon cage, 24 h before testing. The procedure for the modified stress-induced hyperthermia was adapted from Van der Heyden *et al.* and based on the procedure introduced by Borsini *et al.*[36,37] For this assay, the body temperature was measured for each mouse at t = 0 min (T_1) and t = +15 min (T_2). Albino Swiss mice were placed into a new cage immediately following T_1, with the difference in temperature (T_2–T_1) used as the measure of stress-induced hyperthermia. The pilot studies of Spooren demonstrated that a T_2–T_1 interval of 15 min is optimal for assay of SIH.[38] A comparison between T_1 in vehicle-treated mice and those administered with test compound was used to determine whether the agent affects the body temperature alone. The rectal temperature was measured to the nearest 0.1 °C by a Physitemp Thermalert Thermometer, TH-5, (Clifton, NJ, USA), with the temperature sensor for mice, type T, copper-constantan thermocouple, Braintree Scientific Inc. The lubricated thermistor probe (2 mm diameter) was inserted 20 mm into the rectum. The mouse was held at the base of the tail during this determination and the thermistor probe was left in place until a constant reading was obtained for 15 s. Compound **7** was administered at the doses 1, 5 and 15 mg kg^{-1} 60 min before test. Neither vehicle used nor the tested doses of the compound had any influence on the basal body temperature, which was between 36 and 37 °C, typically for Albino Swiss mice used in our laboratory. The statistical significance was evaluated by one-way ANOVA followed by Dunnett's *post hoc* analysis.

The procedures were conducted in accordance with the European Communities Council Directive 2010/63/EU and Polish legislation acts concerning animal experimentation. The experiments were approved by II Local Ethics Committee in Krakow by the Institute of Pharmacology, Polish Academy of Sciences in Krakow (no. 181/2016). All procedures were conducted according to the guidelines of the National Institutes of Health Animal Care and Use Committee.

Conclusions

The recently described 5-(1*H*-indole-3-yl)-1-alkylimidazoles are the first examples of low-basicity agonists of the 5-HT_7R serotonin receptor. Several compounds from this group have been discovered as suitable molecular probe candidates, which could be used for both *in vitro* and *in vivo* studies examining the physiology and pathophysiology of the CNS associated with 5-HT_7R.[20] Indole–imidazole derivatives **7** (previously published) and **13** are the closest structural analogues of the commonly used molecular probe 5-CT (**5**). However, compound **5** exhibits a multi-receptor profile, *i.e.*, high affinity for 5-HT_7R, 5-HT_{1A}R, 5-HT_{5A}R and to some extent also 5-HT_6R receptors. The lack of selectivity as well as low blood–brain barrier permeability are the main disadvantages of **5** as a pharmacological tool. The high affinity of **7** and **13** for 5-HT_7R as well as high selectivity over the 5-HT_{1A} receptor (25-fold and 37-fold, respectively, Table 1) are the main advantages of this compound over 5-CT. *In vitro* comparison studies between **5** **7** and **13** demonstrated their similarities (Table 2). Compounds **5** and **7** displayed very good ability to diffuse passively across biological membranes and also significantly inhibited Pgp. For compound **13** slight, not statistically significant Pgp inhibition was observed. Excellent metabolic stability of **5**, **7**, and **13** was also determined, in particular of compound **13**, for which no metabolites were observed after incubation with HLMs and RLMs. A significant difference between **5** and 3-(1-alkyl-1*H*-imidazol-5-yl)-1*H*-indole-5-carboxamides was observed in the *in vitro* assays only in terms of the influence on cytochromes P-450 activity. However, inhibition activity of **7** and **13** was expected herein, as had been previously observed for another imidazole-based 5-HT_7R agonist – compound **6**.[20] Finally, no significant toxicity or mutagenicity was found for **5**, **7** and **13**.

The *in vivo* activity of **7** was confirmed in pharmacological experiments in mice, providing indirect confirmation of blood–brain barrier permeation. Compound **7** was active in the NOR test in mice at a relatively low dose of 1 mg kg^{-1}, which is in agreement with previous results obtained for 5-CT.[39] Moreover, its activity was also observed in the SIH test at 15 mg kg^{-1}.

We report compounds **7** and **13** as a very promising alternatives to 5-CT with comparable *in vitro* receptor affinity, very high-water solubility, similar *in vitro* ADMET properties and a desirable high selectivity over 5-HT_{1A} receptor. Compound **7**, also confirmed *in vivo* activity in novel object recognition and the modified stress-induced hyperthermia assays.

Conflicts of interest

There are no conflicts to declare.

Acknowledgements

The study was partially supported by the grant OPUS 2017/25/B/NZ7/02929 from the Polish National Science Centre.

Notes and references

1 A. Nikiforuk, *CNS Drugs*, 2015, **29**, 265–275.
2 P. B. Hedlund, *Psychopharmacology*, 2009, **206**, 345–354.
3 D. Hoyer, J. P. Hannon and G. R. Martin, *Pharmacol., Biochem. Behav.*, 2002, **71**, 533–554.
4 M. Ruat, E. Traiffort, R. Leurs, J. Tardivellacombe, J. Diaz, J. M. Arrang and J. C. Schwartz, *Proc. Natl. Acad. Sci. U. S. A.*, 1993, **90**, 8547–8551.
5 T. W. Lovenberg, B. M. Baron, L. Delecea, J. D. Miller, R. A. Prosser, M. A. Rea, P. E. Foye, M. Racke, A. L. Slone, B. W. Siegel, P. E. Danielson, J. G. Sutcliffe and M. G. Erlander, *Neuron*, 1993, **11**, 449–458.
6 M. Leopoldo, E. Lacivita, F. Berardi, R. Perrone and P. B. Hedlund, *Pharmacol. Ther.*, 2011, **129**, 120–148.
7 B. De Filippis, V. Chiodi, W. Adriani, E. Lacivita, C. Mallozzi, M. Leopoldo, M. R. Domenici, A. Fuso and G. Laviola, *Front. Behav. Neurosci.*, 2015, **9**, 86.
8 B. De Filippis, P. Nativio, A. Fabbri, L. Ricceri, W. Adriani, E. Lacivita, M. Leopoldo, F. Passarelli, A. Fuso and G. Laviola, *Neuropsychopharmacology*, 2014, **39**, 2506–2518.
9 L. Costa, L. M. Sardone, E. Lacivita, M. Leopoldo and L. Ciranna, *Front. Behav. Neurosci.*, 2015, **9**, 65.
10 R. Canese, F. Zoratto, L. Altabella, P. Porcari, L. Mercurio, F. de Pasquale, E. Butti, G. Martino, E. Lacivita, M. Leopoldo, G. Laviola and W. Adriani, *Psychopharmacology*, 2015, **232**, 75–89.
11 P. B. Hedlund, M. Leopoldo, S. Caccia, G. Sarkisyan, C. Fracasso, G. Martelli, E. Lacivita, F. Berardi and R. Perrone, *Neurosci. Lett.*, 2010, **481**, 12–16.
12 A. Brenchat, X. Nadal, L. Romero, S. Ovalle, A. Muro, R. Sanchez-Arroyos, E. Portillo-Salido, M. Pujol, A. Montero, X. Codony, J. Burgueno, D. Zamanillo, M. Hamon, R. Maldonado and J. M. Vela, *Pain*, 2010, **149**, 483–494.
13 P. Di Pilato, M. Niso, W. Adriani, E. Romano, D. Travaglini, F. Berardi, N. A. Colabufo, R. Perrone, G. Laviola, E. Lacivita and M. Leopoldo, *Rev. Neurosci.*, 2014, **25**, 401–415.
14 A. P. Bento, A. Gaulton, A. Hersey, L. J. Bellis, J. Chambers, M. Davies, F. A. Kruger, Y. Light, L. Mak, S. McGlinchey, M. Nowotka, G. Papadatos, R. Santos and J. P. Overington, *Nucleic Acids Res.*, 2014, **42**, D1083–D1090.
15 A. Brenchat, L. Romero, M. García, M. Pujol, J. Burgueño, A. Torrens, M. Hamon, J. M. Baeyens, H. Buschmann and D. Zamanillo, *Pain*, 2009, **141**, 239–247.
16 E. Lacivita, S. Podlewska, L. Speranza, M. Niso, G. Satala, R. Perrone, C. Perrone-Capano, A. J. Bojarski and M. Leopoldo, *Eur. J. Med. Chem.*, 2016, **120**, 363–379.
17 E. Lacivita, P. De Giorgio, D. Patarnello, M. Niso, N. A. Colabufo, F. Berardi, R. Perrone, G. Satala, B. Duszynska, A. J. Bojarski and M. Leopoldo, *Exp. Brain Res.*, 2013, **230**, 569–582.
18 T. M. Eriksson, S. Holst, T. L. Stan, T. Hager, B. Sjogren, S. O. Ogren, P. Svenningsson and O. Stiedl, *Neuropharmacology*, 2012, **63**, 1150–1160.
19 J. Andries, L. Lemoine, D. Le Bars, L. Zimmer and T. Billard, *Eur. J. Med. Chem.*, 2011, **46**, 3455–3461.
20 A. S. Hogendorf, A. Hogendorf, R. Kurczab, G. Satala, T. Lenda, M. Walczak, G. Latacz, J. Handzlik, K. Kiec-Kononowicz, J. M. Wieronska, M. Wozniak, P. Cieslik, R. Bugno, J. Staron and A. J. Bojarski, *Sci. Rep.*, 2017, **7**, 15.
21 N. M. Barnes and T. Sharp, *Neuropharmacology*, 1999, **38**, 1083–1152.
22 G. Latacz, A. Lubelska, M. Jastrzebska-Wiesek, A. Partyka, A. Sobilo, A. Olejarz, K. Kucwaj-Brysz, G. Satala, A. J. Bojarski, A. Wesolowska, K. Kiec-Kononowicz and J. Handzlik, *Chem. Biol. Drug Des.*, 2017, **90**, 1295–1306.
23 G. Latacz, A. Lubelska, M. Jastrzebska-Wiesek, A. Partyka, K. Kucwaj-Brysz, A. Wesołowska, K. Kieć-Kononowicz and J. Handzlik, *Bioorg. Med. Chem. Lett.*, 2018, **28**, 878–883.
24 W. A. Banks, *BMC Neurol.*, 2009, **9**, 5.
25 X. X. Chen, A. Murawski, K. Patel, C. L. Crespi and P. V. Balimane, *Pharm. Res.*, 2008, **25**, 1511–1520.
26 R. Mo, X. Jin, N. Li, C. Y. Ju, M. J. Sun, C. Zhang and Q. N. Ping, *Biomaterials*, 2011, **32**, 4609–4620.
27 G. Cruciani, E. Carosati, B. De Boeck, K. Ethirajulu, C. Mackie, T. Howe and R. Vianello, *J. Med. Chem.*, 2005, **48**, 6970–6979.
28 K. Kucwaj-Brysz, D. Warszycki, S. Podlewska, J. Witek, K. Witek, A. G. Izquierdo, G. Satala, M. I. Loza, A. Lubelska, G. Latacz, A. J. Bojarski, M. Castro, K. Kiec-Kononowicz and J. Handzlik, *Eur. J. Med. Chem.*, 2016, **112**, 258–269.
29 E. H. Kerns and L. Di, *Drug-like properties: concepts, structure design and methods: from ADME to toxicity optimization*, Academic Press, Elsevier, Burlington, MA, 1st edn, 2008.
30 W. J. Zhang, Y. Ramamoorthy, T. Kilicarslan, H. Nolte, R. F. Tyndale and E. M. Sellers, *Drug Metab. Dispos.*, 2002, **30**, 314–318.
31 S. Fluckiger-Isler, A. Baumeister, K. Braun, V. Gervais, N. Hasler-Nguyen, R. Reimann, J. Van Gompel, H. G. Wunderlich and G. Engelhardt, *Mutat. Res.*, 2004, **558**, 181–197.
32 S. J. Ballaz, H. Akil and S. J. Watson, *Neuroscience*, 2007, **149**, 192–202.
33 A. Meneses, *Rev. Neurosci.*, 2014, **25**, 325–356.
34 A. Agarwal, R. K. Jalluri, C. De Witt Blanton Jr. and E. Will Taylor, *Synth. Commun.*, 1993, **23**, 1101–1110.
35 M. Nilsson, S. Hansson, A. Carlsson and M. L. Carlsson, *Neuroscience*, 2007, **149**, 123–130.
36 J. A. Van der Heyden, T. J. Zethof and B. Olivier, *Physiol. Behav.*, 1997, **62**, 463–470.
37 F. Borsini, A. Lecci, G. Volterra and A. Meli, *Psychopharmacology*, 1989, **98**, 207–211.
38 W. Spooren, P. Schoeffter, F. Gasparini, R. Kuhn and C. Gentsch, *Eur. J. Pharmacol.*, 2002, **435**, 161–170.
39 T. Freret, E. Paizanis, G. Beaudet, A. Gusmao-Montaigne, G. Nee, F. Dauphin, V. Bouet and M. Boulouard, *Psychopharmacology*, 2014, **231**, 393–400.